Hydroxynonenal inactivates cathepsin B by forming Michael adducts with active site residues

JOHN W. CRABB,[1,2] JUNE O'NEIL,[2] MASARU MIYAGI,[1] KAREN WEST,[1] AND HENRY F. HOFF[2]

[1]Department of Ophthalmic Research, Cole Eye Institute, Cleveland Clinic Foundation, Cleveland, Ohio 44195, USA
[2]Department of Cell Biology, Lerner Research Institute, Cleveland Clinic Foundation, Cleveland, Ohio 44195, USA

(RECEIVED November 1, 2001; FINAL REVISION December 13, 2001; ACCEPTED December 14, 2001)

Abstract

Oxidation of plasma low-density lipoprotein (oxLDL) generates the lipid peroxidation product 4-hydroxy-2 nonenal (HNE) and also reduces proteolytic degradation of oxLDL and other proteins internalized by mouse peritoneal macrophages in culture. This leads to accumulation of undegraded material in lysosomes and formation of ceroid, a component of foam cells in atherosclerotic lesions. To explore the possibility that HNE contributes directly to the inactivation of proteases, structure-function studies of the lysosomal protease cathepsin B have been pursued. We found that treatment of mouse macrophages with HNE reduces degradation of internalized maleyl bovine serine albumin and cathepsin B activity. Purified bovine cathepsin B treated briefly with 15 μM HNE lost ~76% of its protease activity and also developed immunoreactivity with antibodies to HNE adducts in Western blot analysis. After stabilization of the potential Michael adducts by sodium borohydride reduction, modified amino acids were localized within the bovine cathepsin B protein structure by mass spectrometric analysis of tryptic peptides. Michael adducts were identified by tandem mass spectrometry at cathepsin B active site residues Cys 29 (mature A chain) and His 150 (mature B chain). Thus, covalent interaction between HNE and critical active site residues inactivates cathepsin B. These results support the hypothesis that the accumulation of undegraded macromolecules in lysosomes after oxidative damage are caused in part by direct protease inactivation by adduct formation with lipid peroxidation products such as HNE.

Keywords: Oxidative damage; hydroxynonenal; cathepsin B; Michael adducts; mass spectrometry

Oxidation of plasma low-density lipoprotein (oxLDL) generates lipid oxidation products that have been proposed to play a role in the pathogenesis of atherosclerosis by modulating the expression of inflammatory factors and by creating ligands for macrophage scavenger receptors (Witztum and Steinberg 1991; Podrez et al. 2000). When oxLDL is incubated with macrophages in culture, intracellular degradation appears to be deficient after receptor-mediated endocytosis (Lougheed et al. 1991; Jessup et al. 1992; Hoppe et al. 1994). Long-term incubation of macrophages with oxLDL leads to the accumulation of ceroid, an insoluble protein-lipid product that is a hallmark of foam cell lesions and advanced atherosclerotic plaques (Ball et al. 1986; Yin 1996). In vivo and in vitro inhibition of thiol proteases also can result in the formation of ceroid and lipofuscin-like substances (Ivy et al. 1990). The molecular mechanisms responsible for the poor degradation of oxidized macromolecules in macrophages are not fully understood. One mechanism proposes that cross-linking of substrate proteins by

Reprint requests to: John W. Crabb, Ph.D., Cole Eye Institute (i31), Cleveland Clinic Foundation, 9500 Euclid Avenue, Cleveland, OH 44195, USA; e-mail: crabbj@ccf.org; fax: (216) 445-3670 or Henry F. Hoff, Ph.D., Department of Cell Biology (NC-10), Lerner Research Institute, Cleveland Clinic Foundation, Cleveland, OH 44195, USA; e-mail: hoffh@ccf.org; fax: (216) 444-9404.

Abbreviations: BHT, butylated hydroxytoluene; BSA, bovine serum albumin; CLN, Nα-CBZ-L-lysine *p*-nitrophenyl ester; DTT, dithiothreitol; ESMS, electrospray mass spectrometry; HNE, 4-hydroxy-2-nonenal; LC ESMS, liquid chromatography electrospray mass spectrometry; LDL, low-density lipoprotein; ox-LDL, oxidized LDL; PBS, phosphate-buffered saline; TCA, trichloroacetic acid.

Article and publication are at http://www.proteinscience.org/cgi/doi/10.1110/ps.4400102.

oxidative damage hinders accessibility to proteases (Lougheed et al. 1991; Jessup et al. 1992). Another mechanism proposes that treatment of cells with oxLDL leads to a reduced fusion of endosomes or phagosomes with lysosomes (Hoppe et al. 2001). A third mechanism proposes that specific lysosomal proteases are inactivated by lipid oxidation products generated during the oxidation of LDL (Hoppe et al. 1994; O'Neil et al. 1997). This report shows that the lysosomal protease cathepsin B can be inactivated by the lipid peroxidation product 4-hydroxy-2-nonenal (HNE).

Oxidation of LDL leads to multiple changes in the composition of both the lipid and protein constituents of LDL (Esterbauer et al. 1991; Witztum and Steinberg 1991). Free radical–induced formation of hydroperoxides in the unsaturated fatty acids of cholesterol and phospholipid esters (Esterbauer et al. 1991) results in alkoxyl radical formation and subsequent scission to form a variety of reactive lipid oxidation products including HNE. HNE is created by cleavage of oxidized arachidonic and linoleic esters (Fig. 1) and forms Schiff base linkages with primary amino groups and Michael adducts with Lys, His, and Cys residues and also forms fluorescent cross-links (Esterbauer et al. 1991; Xu et al. 2000). HNE modification induces LDL aggregation (Hoff et al. 1992) and impairs proteasome function via cross-linking and other undetermined mechanisms (Friguet and Szweda 1997; Okada et al. 1999). Previously, we reported that a reversal of Michael additions of HNE to lysine may occur at the low pH that exists in lysosomes after receptor-mediated endocytosis of oxLDL (O'Neil et al. 1997). We hypothesized that HNE, still tethered to apo B by a Schiff base linkage also may form Michael additions with particularly vulnerable proteins such as the lysosomal thiol protease cathepsin B (O'Neil et al. 1997). With or without cross-links, Michael additions from HNE may help explain why oxLDL-treated macrophages show reduced activity of cathepsin B but not reduced activity of cathepsin D, an aspartate protease (Hoppe et al. 1994).

A long-term goal of this research is to determine whether the reduced cathepsin B activity observed in oxLDL-treated macrophages is caused by enzyme inactivation from HNE modification. We show here as a step toward this goal that HNE treatment of macrophages reduces cathepsin B activity. Furthermore, we show that HNE treatment of purified

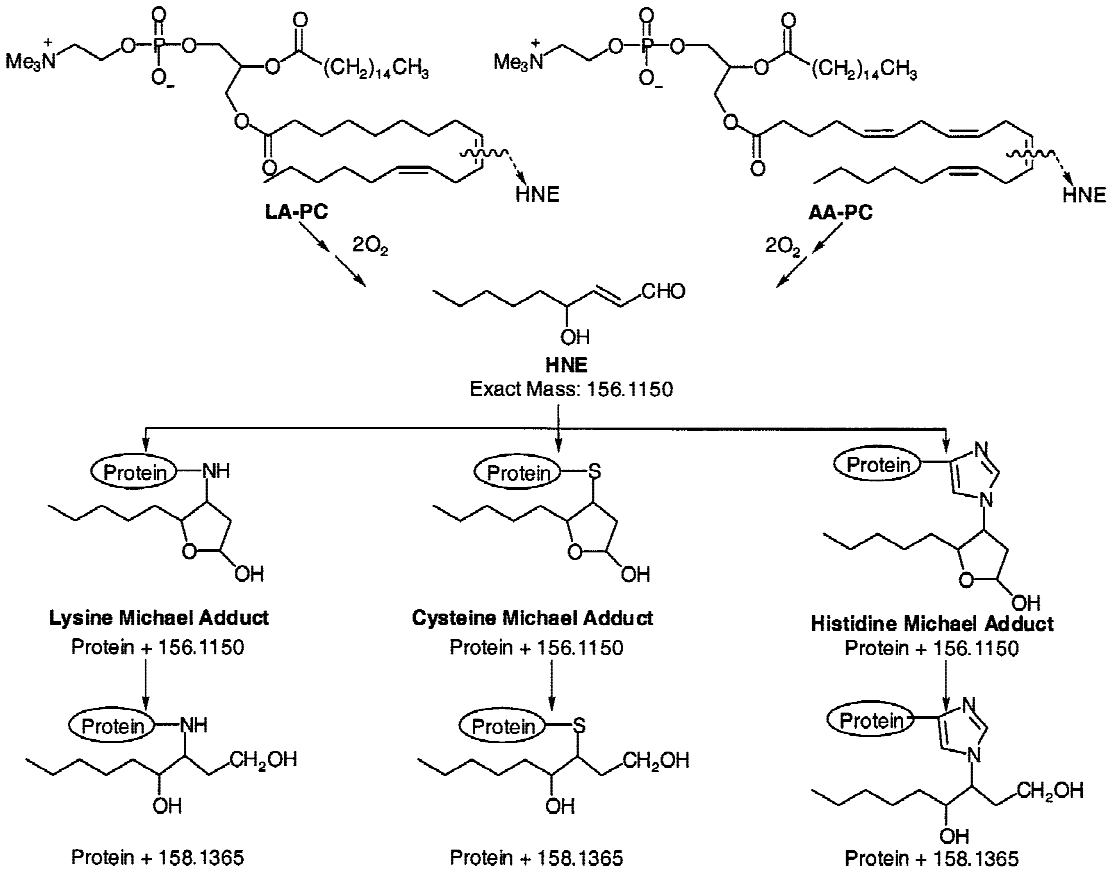

Fig. 1. HNE Michael adducts. HNE (4-hydroxy-2-nonenal) is generated by oxidative cleavage of linoleic (LA) and arachidonic acid (AA) containing phospholipids and can condense with lysine, cysteine, and histidine residues to form Michael adducts. Reduction with $NaBH_4$ stabilizes Michael adducts. The protein mass addition per adduct is indicated. (PC) Phosphatidyl choline; (Me) methyl.

bovine cathepsin B selectively modifies two active site residues, resulting in significant inactivation of the enzyme.

Results

HNE reduces the intracellular degradation of maleyl bovine serine albumin and cathepsin B activity in mouse macrophages

We pretreated mouse peritoneal macrophages with HNE and compared the ability of treated and untreated cells to degrade internalized ^{125}I-maleyl bovine serine albumin (BSA). Under the 3 h reaction conditions used, HNE and oxLDL were able to inhibit degradation of internalized ^{125}I-maleyl BSA by ~35% and 65%, respectively, relative to the untreated control cells (Fig. 2a). In our earlier study of macrophages pretreated with oxLDL for 24 h, reduction in degradation of internalized macromolecules was accompanied by 65%–80% reduction in the activity of cathepsin B (Hoppe et al. 1994). Here, we measured cathepsin B activity after HNE treatment of macrophages and found ~40% reduction in activity relative to untreated cells (Fig. 2b). In this set of experiments, cells pretreated with oxLDL showed approximately a 56% reduction in cathepsin B activity (Fig. 2b). To rule out the possibility that cytotoxicity of HNE or oxLDL reduced degradation of maleyl BSA by modulating protein synthesis, cells were treated with ^{35}S-methionine during incubation with HNE or oxLDL. No significant reduction in protein synthesis was detected (Fig. 2c). Cells were also pretreated with ^{14}C-adenine to monitor for cytotoxicity by measuring release into the media from cell membrane rupture. No significant increase in the release of labeled adenine was found in macrophages treated with up to 50 μM HNE or 100 μg/mL oxLDL (data not shown).

HNE inactivates purified bovine cathepsin B and generates covalent adducts

When purified bovine cathepsin B was treated for 1 h with 15μM HNE, approximately a 76% reduction in enzymatic activity was observed relative to control incubations without HNE (79% and 74% reduction in two separate experiments). No loss of protease activity occurred when the proenzyme was incubated with HNE, but prolonged incubation of the activated cathepsin B in the absence of substrate resulted in self-destruction and complete loss of activity (data not shown). HNE treatment of cathepsin B was terminated after 15 min by addition of 8 M urea, and the preparation was subjected to sodium dodecyl (SDS)–PAGE and Western analysis using an antibody that recognizes HNE Michael adducts (Uchida et al. 1993). Strong HNE immunoreactivity and Coomassie blue staining can be seen at ~30 kD, near the intact mass of active bovine cathepsin B (Fig. 3). Cathepsin B treated with HNE was recognized by the anti-HNE antibody, but the untreated enzyme was not immunoreactive (Fig. 3). Likewise the proenzyme treated with HNE was not immunoreactive (data not shown). These results associate cathepsin B inactivation with HNE covalent modification of the active enzyme.

Identification of Michael adducts in HNE treated cathepsin B

The structural modification induced by HNE treatment of purified bovine cathepsin B was further characterized by mass spectrometry after borohydride reductive stabilization

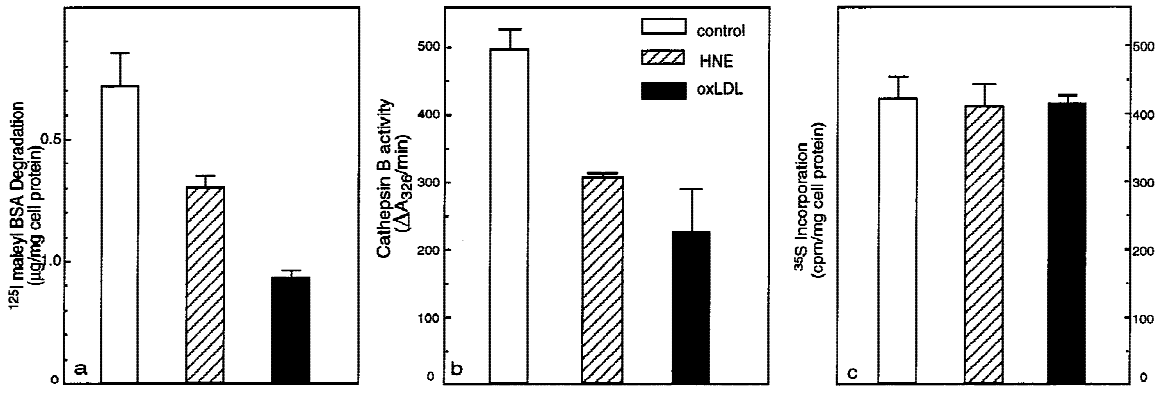

Fig. 2. HNE reduces degradation of maleyl BSA and lowers cathepsin B activity in mouse macrophages. Mouse peritoneal macrophages were incubated for 3 h with media containing one of the following: 150 μg/mL oxLDL, 25 μM HNE in 0.5% ethanol, or 0.5% ethanol (control). After this preincubation, the following analyses were performed. (*a*) Cells were washed three times with fresh media and then incubated with media containing 20 μg/mL of ^{125}I-maleyl BSA. After 2.5 h, the amounts of TCA-soluble label in the conditioned media were determined as described in Materials and Methods. (*b*) Cathepsin B activity in cell lysates was determined as described in Materials and Methods. (*c*) Cells were treated with ^{35}S-methionine during the incubation with HNE or oxLDL to evaluate potential cytotoxicity and reduced protein synthesis. No significant cytotoxicity was detected under the conditions used. The data in each panel represent the average and standard deviation of triplicate determinations. (HNE) 4-hydroxy-2 nonenal; oxLDL: oxidation of plasma low-density lipoproteins.

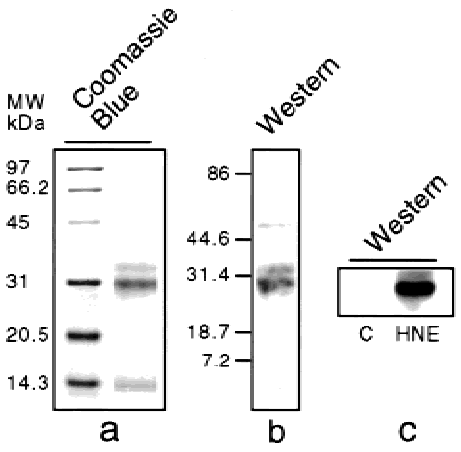

Fig. 3. SDS-PAGE and Western analysis of HNE-modified bovine cathepsin B. Activated bovine cathepsin B was incubated for 1 h with 15 μM HNE and then subjected to SDS-PAGE (~1 μg/lane) and Western analysis using a rabbit polyclonal antibody to HNE adducts (Uchida et al. 1993). (*a*) Coomassie blue-stained gel and (*b*) Western blot of the HNE-treated cathepsin B preparation used for structural analysis by mass spectrometry. (*c*) Western blot of HNE-treated and untreated ([C] control) bovine cathepsin B.

of the preparation. Peptide mass mapping by liquid chromatography electrospray mass spectrometry (LC ESMS) analysis of tryptic peptides from HNE-modified and *S*-carboxyamidomethylated cathepsin B (Fig. 4) provided identification of peptides accounting for ~75% of the protein sequence (Table 1). The AT and BT annotations in the figures and table refer to tryptic peptides from the A-chain and B-chain of cathepsin B, respectively, with associated numbers referring to the specific tryptic peptide ordered sequentially from the N terminus. A mass addition of 158.1 is characteristic of reduced HNE Michael adducts (Fig. 1). Relative to the calculated masses of the unmodified peptides (Table 1) two such peptides were detected by LC ESMS analysis, namely, AT4 (DQGSCG SCWAFGAVEAISDR) and BT10 (SGVYQHVSGEIMG GHAIR). Both peptides were detected in multiple chromatography fractions, suggesting possible conformational differences. Both AT4 and BT10 also were detected without Michael adducts, indicating that the 8-min HNE treatment did not yield quantitative modification of the intact protein. No other peptides with Michael adducts were observed by LC ESMS. In addition, no other anti-HNE immunoreactive peptides were detected by antibody dot blot analysis of chromatography fractions in separate RP HPLC of tryptic digests of HNE-modified cathepsin B (not shown).

To identify HNE-modified amino acids, we subfragmented modified AT4 with chymotrypsin and modified BT10 was cleaved with V8 protease, and then analyzed by nanoelectrospray MS/MS without additional chromatography. Subfragmentation was necessary to obtain complete MS/MS sequence coverage of the modified peptides. Two

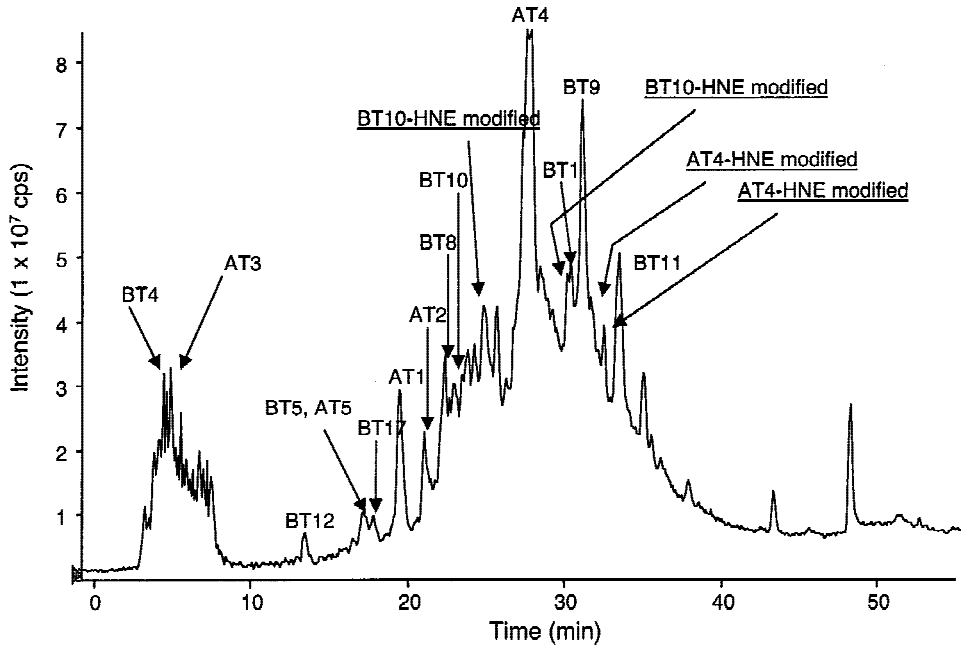

Fig. 4. LC ESMS of tryptic peptides from HNE-modified cathepsin B. Purified bovine cathepsin B was modified with HNE and digested with trypsin, and LC ESMS was performed with a PE Sciex API 3000 triple quadrupole mass spectrometer as described in Materials and Methods. The elution positions of identified tryptic peptides are indicated in the total ion current and summarized in Table 1. HNE-modified peptides were detected by a mass addition of 158.1. (AT) and (BT) Tryptic peptides from the A and B chains of cathepsin B, respectively.

Table 1. *Peptides identified by LC ESMS from HNE-modified cathepsin B*

Peptides	Sequence position	Retention time (min)	Molecular mass		Error[a] (Da)	Sequence
			Calculated	Observed		
Cathepsin B, A-chain tryptic peptides						
AT1	1–8	20.2	933.4	933.8	0.4	LPESFDAR
AT2*[b]	9–18	21.7	1271.6	1271.9	0.3	EQWPNCPTIK
AT3	19–21	5.6	416.2	416.4	0.2	EIR
AT4**	22–41	28.0	2173.3av	2173.4	0.1	DQGSCGSCWAFGAVEAISDR
AT4-HNE modified*	22–41	32.1, 32.7	2274.4av	2274.0	0.4	DQGSCGSCWAFGAVEAISDR
AT5*	42–47	17.8	742.3	742.5	0.2	ICIHSN
Cathepsin B, B-chain tryptic peptides						
BT1****	1–36	30.4	3970.4av	3970.4	0	VNVEVSAEDMLTCCGGECGDGCNGGFPSGAWNFWTK
BT2	37–37	NS	146.1	NS	—	K
BT3***	38–78	ND	4447.9av	ND	G	GLVSGGLYNSHVGCRPYSIPPCEHHVNGSRPPCTGEGDTPK
BT4*	79–81	5.4	393.2	393.4	0.2	CST
BT5	82–92	17.7	1287.5	1287.9	0.4	FWTKKGLVSGG
BT6	93–95	ND	390.2	ND	—	EDK
BT7*	96–109	18.3	1598.7	1598.8	0.1	HFGCSSYSVANNEK
BT8	110–117	22.7	995.5	995.6	0.1	EIMAEIYK
BT9	118–135	31.5	2006.3av	2006.3	0	NGPVEGAFSVYSDFLLYK
BT10	136–153	22.9	1898.1av	1897.8	0.3	SGVYQHVSGEIMGGHAIR
BT10-HNE modified	136–153	25.4, 30.3	2056.2	2056.8	0.4	SGVYQHVSGEIMGGHAIR
BT11	154–183	33.8	3430.7av	3430.6	0.1	ILGWGVENGTPYWLVGNSWNTDWGDNGFFK
BT12	184–186	14.4	400.3	400.4	0.2	ILR
BT13**	187–204	ND	1961.2av	ND	—	GQDHCGIESEIVAGMPCT

Bovine cathepsin B peptides identified by LC ESMS in Fig. 4 are listed by subunit, tryptic peptide, residues, total ion current retention time, calculated and observed masses, and amino acid sequences. Calculated masses are monoisotopic values unless indicated as chemical average masses (av). Error refers to the difference between the observed and calculated masses. The number of asterisks (*) indicates the number of carboxyamidomethyl cysteine residues included in the calculated peptide mass values. (LCESMS) liquid chromatography electrospray mass spectrometry; (HNE) 4-hydroxy-2-nonenal; (G) glycopeptide; (NS) not scanned; (ND) not detected.

predicted chymotryptic cleavage products from HNE-modified AT4 were observed: singly charged m/z 1157.7 and doubly charged m/z 568.6 (Fig. 5). Observed m/z 1157.7 is consistent with calculated MH^+ 1157.8 for the N-terminal AT4 fragment DQGSCGSCW containing one carboxyamidomethyl Cys plus a mass addition of 158.1. The b series of ions from MS/MS analysis of m/z 1157.7 clearly showed that Cys 26 is carboxyamidomethylated and that the Michael adduct is associated with Cys 29 (Fig. 5A). Observed m/z 568.6 agrees well with calculated MH^{+2} 568.7 for the AT4 fragment AFGAVEAISDR with no modifications; MS/MS analysis confirmed the identity of this peptide and its lack of modifications (Fig. 5B). Two doubly charged V8 protease cleavage products, m/z 532.2 and m/z 507.4, were observed from modified BT10 (Fig. 6). Observed m/z 507.4 is consistent with MH^{+2} 507.5 for the C-terminal BT10 fragment IMGGHAIR containing a mass addition of 158.1, and MS/MS analysis of this peptide showed that the HNE Michael adduct is on His 150 (Fig. 6A). Observed m/z 532.2 from BT10 fragment SGVYQHVSGE (calculated MH^{+2} = 532.3) was sequenced and confirmed to contain no modifications (Fig. 6B). Two chromatography fractions contained modified BT10 (Fig. 4), and both yielded the same MS/MS sequence results after subfragmentation with V8 protease (Fig. 6). No evidence for neutral loss of HNE from the modified peptides was apparent during MS/MS analysis.

Discussion

In this study, we found that HNE mimics oxLDL in its ability to reduce intracellular degradation of maleyl BSA and impair cathepsin B activity in macrophages. Furthermore, we have shown that HNE inactivates purified cathepsin B by forming active site Michael adducts. Cathepsin B is a lysosomal thiol protease with papain-like activity that plays a major role in intracellular protein degradation (Illy et al. 1997). The sequence of the bovine enzyme contains 335 amino acids and exhibits a calculated mass of 36,661 Dalton in its precursor form and 251 amino acids and a calculated mass of 27,252 Dalton in its mature, active form (Meloun et al. 1988) The active protease is a disulfide-bonded glycoprotein composed of an A chain (or light chain) of 47 residues and a B chain (or heavy chain) of 204 residues. The X-ray crystal structure of bovine cathepsin B has been determined (Fig. 7), and several critical active site residues have been identified (Yamamoto et al. 2000). The enzyme is unique among lysosomal cysteine proteases in functioning as both an endopeptidase and a peptidyldipeptidase. This unusual carboxypeptidase activity has been re-

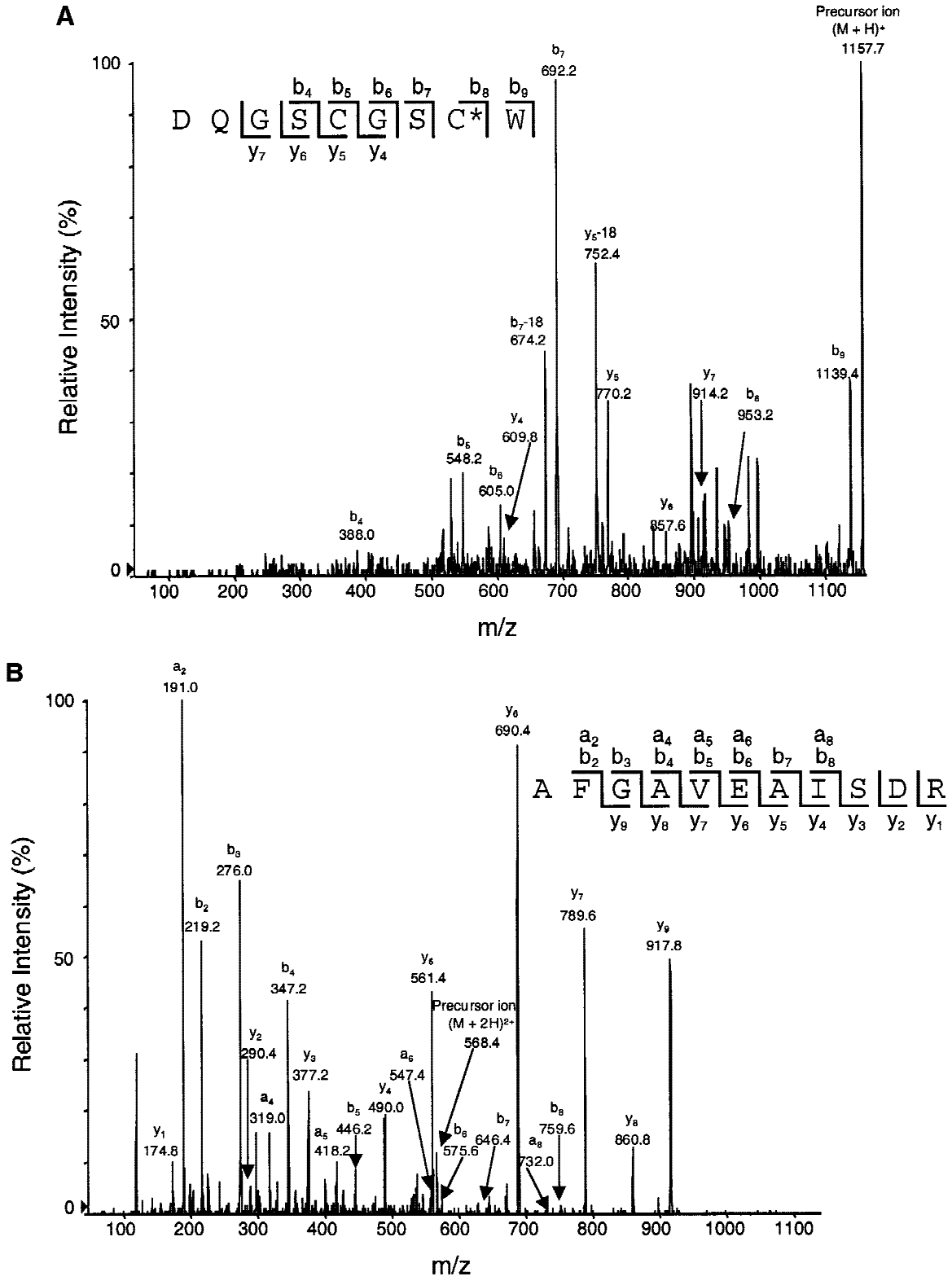

Fig. 5. MS/MS spectra of the HNE-modified active site cysteine peptide. Nanoelectrospray MS/MS spectra are shown for chymotryptic peptides generated from HNE-modified tryptic peptide AT4 (DQGSCGSC*WAFGAVEAISDR): (*A*) singly charged precursor m/z 1157.7 from DQGSCGSC*W; (*B*) doubly charged precursor m/z 568.6 from AFGAVEAISDR. A Michael adduct was found only on the active site cysteine ([asterisk] A-chain Cys 29).

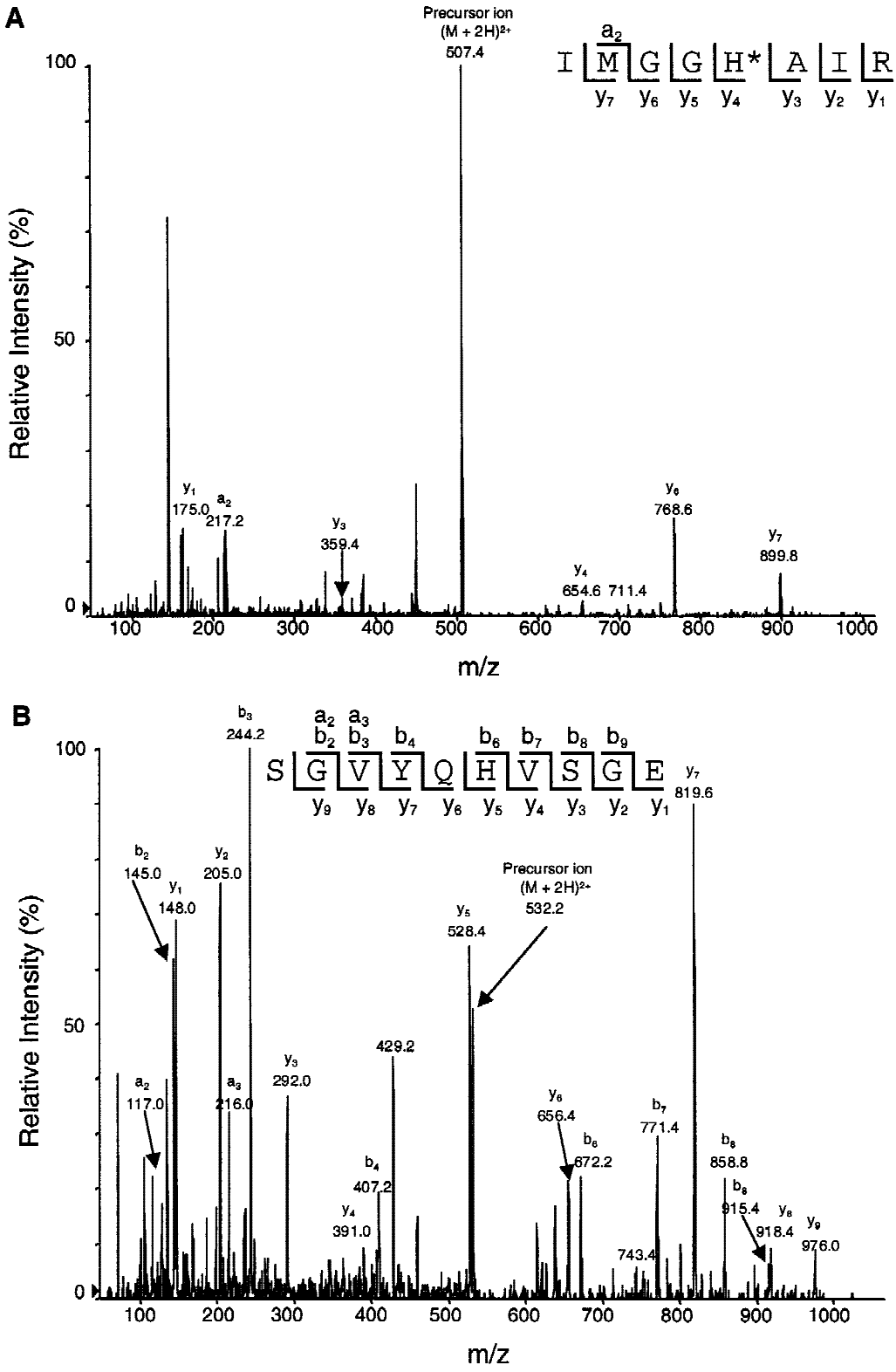

Fig. 6. MS/MS spectra of the HNE-modified active site histidine peptide. Nanoelectrospray MS/MS spectra are shown for V8 protease peptides generated from HNE-modified tryptic peptide BT10 (SGVYQHVSGEIMGGH*AIR): (*A*) doubly charged precursor m/z 532.2 from IMGGH*AIR; (*B*) doubly charged precursor and m/z 507.4 from SGVYQHVSGE. A Michael adduct was found only on the active site histidine ([asterisk] B-chain His 150).

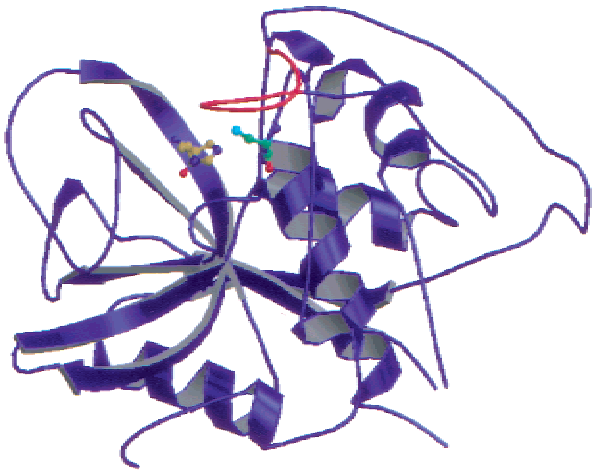

Fig. 7. The three-dimensional structure of cathepsin B. The structure of bovine spleen procathepsin B (Yamamoto et al. 2000) is shown with the active site cysteine and histidine residues that are modified by HNE shown in green and yellow, respectively. Also highlighted in red is the occluding loop (residues 105–125) associated with cathepsin B carboxypeptidase activity (Illy et al. 1997). The structure was drawn using Insight II software (Biosym Technologies), and the PDB coordinates 1QDQ for bovine cathepsin B were obtained from the Structure database, NCBI.

ported to be the result of an occluding loop (Fig. 7), which prevents extended substrates from binding to the enzyme (Illy et al. 1997). Deletion of this loop in mutants leads to loss of exopeptidase activity (Illy et al. 1997). In bovine cathepsin B, the side chain amide of Gln 23 and the backbone amide of Cys 29 in the A chain form an oxyanion hole thought to stabilize reaction intermediates, and Cys 29 and His 150 in the B chain (His 199 in procathepsin B) form a thiolate-imidazolium ion pair that appears to lower the pKa of Cys 29 to 3.4 in the substrate-free enzyme (Yamamoto et al. 2000; Willenbrock and Brocklehurst 1984). The location of Cys 29 and His 150 is highlighted within the cathepsin B structure in Figure 7. During cathepsin B catalyzed hydrolysis, an acyl-enzyme intermediate is thought to form from nucleophilic attack of the Cys 29 thiol on the carbonyl carbon of the scissile amide of the peptide substrate, with a concomitant decrease in the pKa of His 150 to ~4 that facilitates subsequent deacylation (Storer and Menard 1994). HNE modification of either Cys 29 or His 150 would disrupt this enzyme reaction mechanism. Under the pH 4.5 reaction conditions used in this study, we speculate that HNE reacts first with Cys 29, which causes a significant decrease in the pKa of His 150, rendering His 150 also susceptible to electrophilic attack by HNE. Whether both Cys 29 and His 150 are modified in the same cathespsin B molecule is not clear as unmodified peptides containing these residues were detected (Table 1). Such a mechanism of selective HNE modification could have an impact on the activity of thiol proteases in the acidic lysosomal environment.

HNE is an especially cytotoxic lipid oxidation product that generates not only Schiff base and Michael adducts (Fig. 1) but also fluorescent cross-links (Xu et al. 2000). HNE-derived cross-links have been credited with inhibiting proteasome function (Friguet and Szweda 1997) and may contribute to the fluorescence seen in atherosclerotic plaques and age-related lipofuscin granules (Ball et al. 1986; Kikugawa and Beppu 1987). A variety of enzymes has been shown to be susceptible to inactivation from HNE active site adducts including glucose-6-phosphate dehydrogenase (Szweda et al. 1993), glyceraldehyde-3-phosphate dehydrogenase (Uchida et al. 1993), glutathione *S*-transferase (Mitchell et al. 1995), glutathione reductase (Vander Jagt et al. 1997), interleukin 1B converting enzyme (Davis et al. 1997), and aldose reductase (Del Corso et al. 1998). These earlier studies used a variety of tools to assess HNE adduct formation, including quantification of thioether linkages between HNE and thiols using Raney nickel (Uchida and Stadtman 1992), immunochemical detection with anti-HNE antibodies (Uchida et al. 1993), and mass spectrometry. We used a combination of immunochemical and mass spectrometric methods in the present study of cathepsin B. Preventing autodigestion and stabilizing Michael adducts by sodium borohydride reduction were important technical aspects of our structural characterization of this thiol protease.

In summary, HNE or oxLDL treatment of macrophages inhibits intracellular degradation of macromolecues and reduces cathepsin B activity. HNE treatment of purified bovine cathepsin B results in selective modification of active site residues Cys 29 (A chain) and His 150 (B chain), with the generation of Michael adducts and significantly reduced enzyme activity. Notably, others have established the presence of HNE Michael adducts in oxLDL (Esterbauer et al. 1991; Bolgar et al. 1996). Overall, these results support the hypothesis that specific lysosomal proteases are inactivated by HNE generated during oxidation of LDL.

Materials and methods

Materials

Bovine spleen cathepsin B (EC 3.4.22.1), Nα-CBZ-L-lysine *p*-nitrophenyl ester, fatty acid–free bovine serum albumin, butylated hydroxytoluene, trichloroacetic acid, and dithiothreitol were purchased from Sigma Chemical Co. Carrier-free $Na^{125}I$ and ^{14}C-adenine were from ICN, Roswell Park Memorial Institute media (RPMI-1640) was from Whittaker Bioproducts Inc., and fetal calf serum was from Gibco Laboratories. Tissue culture plates were obtained from Costar; C57BL/6 mice (16–20 weeks of age) from Charles River Laboratory; and polyvinylidene difluoride (PVDF) membrane was from Amersham-Pharmacia Biotech. HNE and rabbit polyclonal antiserum to HNE were kind gifts from Drs. Lawrence M. Sayre and Luke I. Szweda, respectively, Case Western Reserve University, Cleveland, OH.

Degradation of maleyl bovine serum albumin by macrophages in culture

LDL was isolated from fresh plasma obtained from the Cleveland Clinic Blood Bank and oxidized with $CuSO_4$ as described elsewhere (Hoppe et al. 1994). BSA was subjected to maleylation (Haberland and Fogelman 1985), labeled with $Na^{125}I$, and used as a ligand for receptor-mediated endocytosis. Mouse peritoneal macrophages were harvested 2–3 days after thioglycollate stimulation of female C57BL/6 mice by peritoneal lavage with ice-cold phosphate-buffered saline (PBS). Primary cultures were prepared at a density of 10^6 cells/16-mm-diameter well in RPMI-1640 containing 10% fetal calf serum and used 48 h after plating (Hoppe at al. 1994). Cells were treated with HNE or oxLDL for 3 h, washed two times with PBS to remove oxLDL or HNE, then incubated with ^{125}I-maleyl BSA and media assayed for trichloroacetic acid–soluble, noniodine degradation products essentially as described elsewhere (Hoppe et al. 1994). Cells were washed three times with PBS, dissolved in 0.1 N NaOH, and assayed for protein content using the bicinchoninic acid assay and BSA as a standard (Pierce Chemicals). Cytotoxicity was determined by measuring the incorporation of ^{35}S-methionine into proteins, and by determining the release of ^{14}C-adenine from cells (Coffey et al. 1995). In the latter technique, macrophages were first incubated with media containing ^{14}C-adenine (0.2 μ Ci/mL) for 12 h, washed with media, and then incubated with HNE or oxLDL for 3 h at 37°C. The amount of radiolabel present in the conditioned media as a result of release from cells then was measured.

Preparation of macrophage cell extracts

Mouse peritoneal macrophages were assayed for cathepsin B activity as previously described (Hoppe et al. 1994). Briefly, after incubation with HNE or oxLDL, macrophage monolayers were washed twice with PBS, scraped with a rubber policeman, pelleted by centrifugation at 2000*g* for 10 min and resuspended in 1 mL of buffer. The cells then were ruptured by passing 10 times through a 30-gauge needle, followed by 10 cycles of freezing and thawing, and finally by two 15-sec bursts of sonication (Hoppe et al. 1994). The homogenates were spun at 5000*g* to remove particulate matter, and supernatant fractions were collected and defined as cell extracts.

Enzyme assay for cathepsin B activity

The thiol protease activity of cell extracts and purified cathepsin B preparations was assayed by the Nα-CBZ-L-lysine *p*-nitrophenyl ester (CLN) procedure (Hoppe et al. 1994). Briefly, bovine cathepsin B was activated by incubating the proenzyme for 15 min at 37°C in 0.2 M Na acetate at pH 4.5 containing 2 mM DTT-EDTA. The activated enzyme was treated with 15 μM HNE for periods of up to 60 min. An aliquot of the mixture of activated enzyme with or without HNE was adjusted to 1 mL with the same buffer, and the enzyme reaction was initiated by addition of CLN to a final concentration of 0.5 mM. Cathepsin B activity at 37°C was expressed as change in absorbance at 326 nm wavelength per min because of hydrolysis of CLN.

HNE modification of bovine cathepsin B, sodium borohydride reduction, alkylation, and proteolytic digestions

Purified and activated bovine cathepsin B (~8 nmole based on vendor quantification) in 250 μL of 100 mM sodium acetate at pH 4.5 and 1 mM DTT-EDTA was added to 1.6 μmole HNE dissolved in 25 μL of ethanol. After an 8-min incubation at 37°C, 8 M urea in 200 mM ammonium bicarbonate at pH 8.0 (1 mL) was added to stop autoproteolysis, and the preparation was frozen. To stabilize Michael adducts and reduce disulfide bonds, we added 1 M sodium borohydride in 0.1 M NaOH to the HNE-modified protein to a final concentration of 50 mM, and the EDTA concentration was adjusted to 1 mM. After 30 min incubation at room temperature in a fume hood, hydrogen gas bubbling was stopped and ~2.8-fold molar excess of iodoacetamide was added relative to the cysteine content. After a 15-min incubation under argon, the alkylation reaction was stopped by the addition of 1 μmole DTT. The modified cathepsin B was dialyzed exhaustively into 15 mM *N*-ethylmorpholine acetate at pH 8.0, 40% acetonitrile using 1000-MW cutoff Spectrapor dialysis tubing. After dialysis, the modified cathepsin B was quantified by amino acid analysis and recovery determined to be ~109 μg (~4 nmole). HNE-modified and *S*-carboxyamidomethylated cathepsin B (2.1 nmole) was digested with 1.8 μg of trypsin (Promega) in 15 mM *N*-ethylmorpholine acetate at pH 8.0, 40% acetonitrile at 37°C for 16 h. Subfragmentation of tryptic peptides with V8 protease or chymotrypsin (0.1 μg protease) was in 10 mM ammonium bicarbonate containing 20% acetonitrile at 25°C for 12 h (Crabb et al. 1986).

Amino acid analysis, electrophoresis, and Western blot analysis

Phenylthiocarbamyl amino acid analysis was performed using an Applied Biosystems model 420H/130/920 automated analysis system (Crabb et al. 1998a). SDS-PAGE was performed on 12% acrylamide gels using a Mini-Protein II slab gel system (Bio-Rad) and visualized by Coomassie blue staining. For Western analyses, the gels were blotted to PVDF membranes and probed with rabbit polyclonal antibodies to Michael adducts (Uchida et al. 1993). Immunoreactivity was detected by chemiluminescence (Amersham-Pharmacia Biotech).

Mass spectrometry

ESMS and liquid chromatography ESMS (LC ESMS) were performed with a Perkin-Elmer Sciex API 3000 triple quadrupole mass spectrometer equipped with an ionspray source (Crabb et al. 1998b). Nitrogen was used as the nebulization gas (at 40 p.s.i.) and curtain gas and was supplied from a nitrogen dewar. For LC ESMS, the cathepsin B tryptic digest was diluted twofold with 0.1% trifluoroacetic acid and ~1 nmole (~27 μg) chromatographed on a 5 μm Vydac C18 column (1.0 × 150 mm) using an Applied Biosystems model 140D HPLC system, aqueous acetonitrile/propanol/trifluoroacetic acid solvents and a linear gradient of 2%–80% acetonitrile over 60 min at a flow rate of 40 μL/min. The column eluant was split with 25% directed to the mass spectrometer. The remainder of the eluant was collected manually in fractions by monitoring the total ion current. A scan range of m/z 350–2200 in the positive ion mode was used with 0.2-a.m.u. steps, 0.5-msec dwell time per step, 70-V orifice potential, and 4900-V ionspray.

Nanoelectrospray MS/MS was performed with a nanoelectrospray interface (MDS Protana) attached to the Perkin-Elmer Sciex API 3000 triple quadrupole mass spectrometer. Select chromatography fractions from LC ESMS (~5 μL) were placed in gold-coated glass capillaries (4-μm outlet; New Objectives, Inc.), and the samples were infused into the mass spectrometer with 1000–1500 V applied to the capillary and orifice potential set at 40 V.

Precursor ions were selected in the first quadrupole (Q1) and collision-induced dissociation effected with nitrogen gas in the second quadrupole (Q2). Product ion spectra were obtained by scanning the third quadrupole (Q3) using a step size of 0.2 Dalton and 0.5 msec dwell time per step in the positive ion mode. The Q1 resolution was lowered to allow transmission of M^{+1} precursor ions into Q2; Q3 was kept at unit mass resolution.

Acknowledgments

This work was supported in part by NIH grants EY06603 and HL53315, a Research Center Grant from the Foundation Fighting Blindness, Hunt Valley, MD, and funds from The Cleveland Clinic Foundation. We thank Xiaorong Gu and Drs. Sanjoy Bhattacharya and Barnali Neel Chaudhuri for assistance with illustrations and Drs. G. Hoppe, M. Kinter, and L. Sayre for reviewing the manuscript before publication.

The publication costs of this article were defrayed in part by payment of page charges. This article must therefore be hereby marked "advertisement" in accordance with 18 USC section 1734 solely to indicate this fact.

References

Ball, R.Y., Bindman, J.P., Carpenter, K.L.H., and Mitchenson, M.J. 1986. Oxidised low density lipoprotein induces ceroid accumulation by murine peritoneal macrophages in vitro. *Atherosclerosis* **60:** 173–181.

Bolgar, M.S., Yang, C.Y., and Gaskell, S.J. 1996. First direct evidence for lipid/protein conjugation in oxidized human low density lipoprotein. *J. Biol. Chem.* **271:** 27999–28001.

Crabb, J.W., Armes, L.G., Carr, S.A., Johnson, C.M., Roberts, G.D., Bordoli, R.S., and McKeehan, W.L. 1986. The complete primary structure of prostatropin, a prostate epithelial cell growth factor. *Biochemistry* **25:** 4988–4993.

Crabb, J.W., Carlon, A., Chen, Y., Goldflam, S., Intres, R., West, K., Hulmes, J.D., Kapron, J.T., Luck, L.A., Horwitz, J., and Bok, D. 1998a. Structural and functional characterization of recombinant human cellular retinaldehyde-binding protein. *Protein Sci.* **7:** 746–757.

Crabb, J.W., Nie, Z., Chen, Y., Hulmes, J.D., West, K.A., Kapron, J.T., Ruuska, S.E., Noy, N., and Saari, J.C. 1998b. Cellular retinaldehyde-binding protein ligand interactions; Gln210 and Lys221 are in the retinoid-binding pocket. *J. Biol. Chem.* **273:** 20712–20720.

Coffey, M.D., Cole, R.A., Colles, S.M., and Chisolm, G.M. 1995. In vitro cell injury by oxidized low density lipoprotein involves lipid hydroperoxide-induced formation of alkoxyl, lipid and peroxyl radicals. *J. Clin. Invest.* **96:** 1866–1873.

Davis, D.W., Hamilton, R.F., and Holian, A. 1997. 4-Hydroxynoneal inhibits interleukin-1β converting enzyme. *J. Interferon Cytokine Res.* **17:** 205–219.

Del Corso, A., Dal Monte, M., Vilardo, P.G., Cecconi, I., Moschini, R., Banditelli, S., Cappiello, M., Tsai, L., and Mura, U. 1998. Site-specific inactivation of aldose reductase by 4-hydroxynonenal. *Arch. Biochem. Biophys.* **350:** 245–248.

Esterbauer, H., Schaur, R.G., and Zollner, H. 1991. Chemistry and biochemistry of 4-hydroxynonenal, malonaldehyde and related aldehydes. *Free Radic. Biol. Med.* **11:** 81–128.

Friguet, B. and Szweda, L.I. 1997. Inhibition of the multicatalytic proteinase (proteasome) by 4-hydroxy-2-nonenal cross-linked protein. *FEBS Lett.* **405:** 21–25.

Haberland, M.E. and Fogelman, A.M. 1985. Scavenger receptor-mediated recognition of maleyl bovine plasma albumin and the demaleylated protein in human monocyte macrophages. *Proc. Natl. Acad. Sci.* **82:** 2693–2697.

Hoff, H.F., Whitaker, T.E., and O'Neil, J. 1992. Oxidation of low density lipoprotein leads to particle aggregation and altered macrophage recognition. *J. Biol. Chem.* **267:** 602–609.

Hoppe, G.B., O'Neil, J., and Hoff, H.F. 1994. Inactivation of lysosomal proteases by oxidized LDL is partially responsible for its poor degradation by mouse peritoneal macrophages. *J. Clin. Invest.* **94:** 1506–1512.

Hoppe, G., Pennock, E., Marmorstein, A., and Hoff, H.F. 2001. Oxidized low density lipoprotein-induced inhibition of processing of photoreceptor outer segments by RPE. *Invest. Ophthalmol. Vis. Sci.* **42:** 2714–2720.

Illy, C., Quraishi, O., Wang, J., Purisima, E., Vernet, T., and Mort, J.S. 1997. Role of the occluding loop in cathepsin B activity. *J. Biol. Chem.* **272:** 1197–1202.

Ivy, G.O., Kanai, S., Ohta, M., Smith, G., Sato, Y., Kobayashi, M., and Kitani, K. 1990. Lipofuscin-like substances accumulate rapidly in brain, retina and internal organs with cysteine protease inhibition. In *Lipofuscin and ceroid pigments*. (ed. E.A. Porta), pp. 31–47. Plenum Press, New York.

Jessup, W., Mander, E.L., and Dean, R.L. 1992. The intracellular storage and turnover of apolipoprotein B of oxidized LDL in macrophages. *Biochim. Biophys. Acta* **1126:** 167–177.

Kikugawa, K. and Beppu, M. 1987. Involvement of lipid oxidation products in the formation of fluorescent and cross-linked proteins. *Chem. Phys. Lipids* **44:** 277–296.

Lougheed, M., Zhang, H., and Steinbrecher, U.P. 1991. Oxidized low density lipoprotein is resistant to cathepsins and accumulates within macrophages. *J. Biol. Chem.* **266:** 14519–14525.

Meloun, B., Baudys, M., Pohl, J., Pavlik, M., and Kostka, V. 1988. Amino acid sequence of bovine spleen cathepsin B. *J. Biol. Chem.* **263:** 9087–9093.

Mitchell, A.E., Morin, D., Lame, M.W., and Jones, A.D. 1995. Purification, mass spectrometric characterization, and covalent modification of murine glutathione S-transferases. *Chem. Res. Toxicol.* **8:** 1054–1062.

Okada, K., Wangpoengrakul, C., Osawa, T., Toyokunit, S., Tanaka, K., and Uchida, K. 1999. 4-Hydroxy-2-nonenal-mediated impairment of intracellular proteolysis during oxidative stress. *J. Biol. Chem.* **274:** 23787–23793.

O'Neil, J., Hoppe, G., Sayre, L., and Hoff, H.F. 1997. Inactivation of cathepsin B by oxidized LDL involves complex formation induced by binding of reactive sites exposed at low pH to thiols on the enzyme. *Free Radic. Biol. Med.* **23:** 215–225.

Podrez, E.A., Febbraio, M., Sheibani, N., Schmitt, D., Silverstein, R., Hajjar, D.P., Cohen, P.A., Frazier, W.A., Hoff, H.F., and Hazen, S.L. 2000. The macrophage scavenger receptor CD36 is the major receptor for LDL recognition following modification by monocyte-generated reactive nitrogen species. *J. Clin. Invest.* **105:** 1095–1108.

Storer, A.C. and Menard, R. 1994. Catalytic mechanism in papain family of cysteine peptidases. *Methods Enzymol.* **244:** 486–500.

Szweda, L.I., Uchida, K., Tsai, L., and Stadtman, E.R. 1993. Inactivation of glucose-6-phosphate dehydrogenase by 4-hydroxy-2-nonenal. Selective modification of an active-site lysine. *J. Biol. Chem.* **268:** 3342–3347.

Uchida, K. and Stadtman, E.R. 1992. Selective cleavage of thioether linkage in proteins modified with 4-hydroxynonenal. *Proc. Natl. Acad. Sci.* **89:** 5611–5615.

———. 1993. Covalent attachment of 4-hydroxynonenal to glyceraldehyde-3-phosphate dehydrogenase. A possible involvement of intra- and intermolecular cross-linking reaction. *J. Biol. Chem.* **268:** 6388–6393.

Uchida, K., Szweda, L.I., Chae, H., and Stadtman, E.R. 1993. Immunochemical detection of 4-hydroxynonenal protein adducts in oxidized hepatocytes. *Proc. Natl. Acad. Sci.* **90:** 8742–8746.

Vander Jagt, D.L., Hunsaker, L.A., Vander Jagt, T.J., Gomez, M.S., Gonzales, D.M., Deck, L.M., and Royer, R.E. 1997. Inactivation of glutathione reductase by 4-hydroxynonenal and other endogenous aldehydes. *Biochem. Pharmacol.* **53:** 1133–1140.

Willenbrock, F. and Brocklehurst, K. 1984. Natural structural variation in enzymes as a tool in the study of mechanism exemplified by a comparison of the catalytic-site structure and characteristics of cathepsin B and papain. *Biochem J* **222:** 805–814.

Witztum, J.L. and Steinberg, D. 1991. Role of oxidized low density lipoprotein in atherogenesis. *J. Clin. Invest.* **88:** 1785–1792.

Xu, G., Liu, Y., and Sayre, L.M. 2000. Polyclonal antibodies to a fluorescent 4-hydroxy-2-nonenal (HNE)-derived lysine-lysine cross-link: Characterization and application to HNE-treated protein and in vitro oxidized low-density lipoprotein. *Chem. Res. Toxicol.* **13:** 406–413.

Yamamoto, A., Tomoo, K., Hara, T., Murata, M., Kitamura, K., and Ishida, T. 2000. Substrate specificity of bovine cathepsin B and its inhibition by CA074, based on the crystal structure refinement of the complex. *J. Biochem.* **127:** 635–643.

Yin, D. 1996. Biochemical basis of lipofuscin, ceroid, and age pigment-like fluorophores. *Free Radic. Biol. Med.* **21:** 871–888.